OPTOELECTRONICS AND ADVANCED MATERIALS – RAPID COMMUNICATIONS Vol. 15, No. 9-10, September-October 2021, p. 498 - 503

Assessing the structural properties of $Ge_xAs_xSe_{1-2x}$ chalcogenide systems through cross-correlated STEM, XRD and micro-Raman studies

O. V. IASENIUC[a], M. S. IOVU[a], A. PANTAZI[b,c], O. A. LAZAR[b], C. C. MOISE[b], M. ENACHESCU[b,d]
[a]*Institute of Applied Physics, Str. Academiei 5, MD-2028 Chisinau, R. Moldova*
[b]*Center for Surface Science and Nanotechnology, University Politehnica of Bucharest, Splaiul Independentei 313, Bucharest, Romania*
[c]*S.C. NanoPRO START MC S.R.L., Mitropolit Antim Ivireanu Street 40, 110310 Pitesti, Romania*
[d]*Academy of Romanian Scientists, Ilfov Street, 3, 50044 Bucharest, Romania*

In this work we present the preparation and structural properties assessment of powder and thin film ternary $Ge_xAs_xSe_{1-2x}$ (x=0.07÷0.30) chalcogenide glasses by cross-correlating different advanced characterization methods: Scanning Transmission Electron Microscopy (STEM), X-Ray diffraction (XRD) and micro-Raman Spectroscopy investigation methods. STEM and XRD showed the amorphous nature of powder samples and the presence of crystalline domains in the deposited thin films. Moreover, XRD unveiled the intermediate range order (IRO) organization in some of the prepared samples through the appearance of the First Sharp Diffraction Peak (FSDP) in their patterns. The micro-Raman study showed the characteristic Raman signature of $Ge_xAs_xSe_{1-2x}$ systems and the effects of composition variation. With the increase of Ge and As fractions, a significant increase in the density of the $Ge(Se_{1/2})_4$ structural units has been observed. Based on all these results, we are providing a thorough insight in the structural arrangements of different $Ge_xAs_xSe_{1-2x}$ compositions, which could enable the control of these systems' physical properties to make them suitable for different applications, such as phase change memory devices.

(Received May 7, 2021; accepted October 7, 2021)

Keywords: Chalcogenide glasses, X-ray diffraction patterns, Micro-Raman spectra, TEM

1. Introduction

In contrast to the crystalline materials which show a long-range order (LRO), described by correlations between the atoms, independently of their distance, the non-crystalline solids preserve a short-range order (SRO) in the range of 0.3-0.5 nm, being characterized by an interatomic correlation in the first coordination sphere of an arbitrary atom. For the amorphous solids with strong covalent networks, the SRO is described by local coordination polygons, such as pyramidal $AsSe_3$, As_2Se_3, and tetrahedral Ge_2Se_3, GeSe, $GeSe_2$ structural units.

For many amorphous semiconductors, such as chalcogenide glasses, this order is shown at longer distances, so-called medium/intermediate range order (MRO/IRO),which extends up to the range of 0.5-1.0 nm [1].The intermediate range order has an extremely important role in the control of covalent glasses properties, which have still many unaddressed questions [2].

Arsenic selenide glasses mixed with Group IV metals (Sn or Ge) lead to the formation of ternary chalcogenide glasses, which besides pyramidal structural units ($AsSe_{3/2}$), also contain tetrahedral structural units, such as $(GeSe_{1/2})_4$ and $Sn(Se_{1/2})_4$. The analysis of the metallic bonds formation and phase separation in the investigated $Ge_xAs_xSe_{1-2x}$ glasses can unveil some of their physical and chemical properties [3]. Ternary $Ge_xAs_xSe_{1-2x}$ chalcogenide glasses are sensitive to light irradiation, e-beam [4] etc., are promising materials for various photonic, electronic and optoelectronic [5] applications due to their high chemical stability, high transmittance in the IR region, high refractive index (n ≈ 2.4÷2.8) and optical nonlinearity [6].

This work focuses on the preparation and structural properties assessment of $Ge_xAs_xSe_{1-2x}$ powder and thin film chalcogenide glasses by cross-correlating different advanced characterization methods, namely STEM, XRD and micro-Raman Spectroscopy.

2. Experimental

2.1. Synthesis of $Ge_xAs_xSe_{1-2x}$ chalcogenides

The bulk chalcogenide glasses of $Ge_xAs_xSe_{1-2x}$ (x = 0.05÷0.30), with the mean coordination number Z = 2.15÷2.90, were synthesized using 6N purity (99.999%) Ge, As and Se elements by conventional melt-quenching method. Appropriate amounts of the initial materials (Ge, As and Se), precisely weighted considering their atomic masses, have been placed and mixed in quartz ampoules, which afterwards have been evacuated and sealed under 10^{-5}Torr vacuum conditions. Subsequently, the resultant mixtures were melted in a rocking furnace at a temperature which was gradually increased at a rate of 1°C/min up to 900°C. This temperature was kept constant for 48 hours in order to ensure the homogenization of the synthesized materials and then the quartz ampoules were slowly quenched to room temperature. Part of the synthetized ingots have been ground into powders with a grain size of about 100 nm and were used for the X-ray and Micro-Raman measurements. Another part of them has been used for the preparing the thin film layers by thermal vacuum evaporation.

Using the obtained bulk $Ge_xAs_xSe_{1-2x}$ chalcogenides, thin film samples with thicknesses of 1÷2 μm were deposited by flash thermal evaporation method in vacuum 10^{-5}Torr on heated glass substrates at 100 °C. The thickness of the thin films was controlled during the deposition process in a vacuum chamber, using the dependence of the thickness on the deposition time and on the mass of the evaporated material. Besides that, the thickness was estimated by the Linnik interferometer.

2.2. Experimental techniques

The micro-Raman studies have been carried out at room temperature by confocal micro-Raman Spectroscopy using a LabRam HR800 system. The Raman spectra were recorded by exposing the specimens during 300 s to a 0.03 mW, 532 nm wavelength green excitation laser and by dispersing the samples' emitted signal on the CCD detector using a 600 lines/mm grating with a spectral resolution around 0.6 cm^{-1}.

The X-ray diffraction (XRD) investigations were performed on a High Resolution SmartLab X-Ray Diffractometer (Rigaku Corporation Tokyo Branch, Japan) using CuK_α radiation (λ = 0.154060 nm). All the diffractograms were recorded at room temperature, on a large range of 2 theta angles (15-80 deg.) with a scanning step of 0.6 degrees. The phase identification was made by referring to the International Center for Diffraction Data – ICDD (PDF-2) database.

The High Resolution-Scanning Transmission Electron Microscopy (HR-STEM) analyses were carried out using a Hitachi HD-2700 STEM system, equipped with Energy Dispersive X-Ray Oxford detector-analyzer. For STEM measurements, the material was dispersed in ethanol solvent, sonicated and deposited onto a standard Cu TEM grid. The STEM images were recorded by using three different detectors, secondary electrons (SE), phase contrast (PhC) and transmission electrons (TE), respectively, at the same location on the sample.

3. Results and discussion

3.1. STEM results

The morphological and structural properties of the prepared $Ge_xAs_xSe_{1-2x}$ chalcogenide glasses in both, powder and thin film, forms have been investigated using Scanning Transmission Electron Microscopy (STEM) technique. In Fig. 1, a set of representative secondary electrons (SE), phase contrast (PhC) and transmission electrons (TE) detectors-based images, recorded on the same location for each type of $Ge_xAs_xSe_{1-2x}$ sample, powder and thin film, respectively, is presented. The SE, PhC and TE detectors-based images are spatially correlated, being recorded on the same location, but each of them shows different, but complementary, sample property information.

As can be observed in Fig. 1a), the surface morphology of the powder sample is described by the presence of flake-shaped particles, having different sizes up to 900 nm. The PhC image revealed by the powder sample (Fig. 1b) does not show significant contrast variations over the investigated area, except for the regions which are evidently thinner as highlighted by TE image (Fig. 1c), indicating a uniform distribution of the three components (Ge, As, Se) into the final material. As expected, the thin film sample exhibited a considerably smoother surface morphology (Fig. 1d). No significant contrast variations were observed in the PhC image (Fig. 1e) for this sample either. As shown by the TE image (Fig. 1d), the investigated film did not reveal any noticeable thickness variations.

Fig. 2 illustrates representative HR-STEM images revealed by $Ge_xAs_xSe_{1-2x}$ powder and thin film samples. The HR-STEM image from Fig. 2a), obtained by transmission electrons detector at x8000K magnification, indicates the amorphous organization of the powder sample, this result being in close correlation with other investigated areas on these specimens. In the HR-STEM images exhibited by the thin film and recorded at x2500K magnification, besides the expected amorphous organization (Fig. 2b), crystalline areas have been also detected in the material as highlighted by the white square marks in Fig. 1c. The two profiles illustrated in Fig. 2 (b, c), have been extracted from the crystalline regions marked with 1 and 2 in Fig. 2c and exhibited inter-planar distances around 3.14 Å and 6.02 Å, respectively.

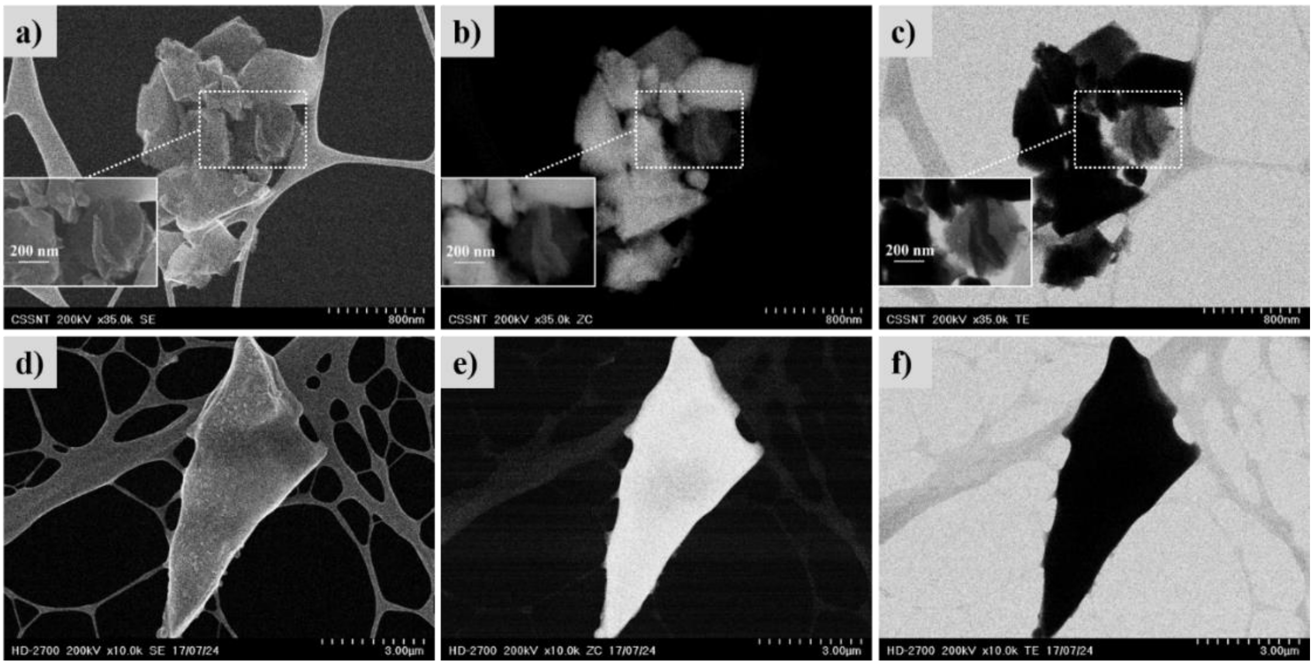

Fig. 1. Representative STEM secondary electrons (SE) – (a, d), phase contrast (PhC) – (b, e) and transmission electrons (TE) – (c, f) images, recorded at the same sample location for both, powder (top) and thin film (bottom) $Ge_xAs_xSe_{1-2x}$ chalcogenides

3.2. X-Ray Diffraction results

The X-Ray diffraction patterns revealed by the $Ge_xAs_xSe_{1-2x}$ (x=0.05÷0.30) chalcogenide glasses, both in powder and thin film forms, are illustrated in Fig. 2 a), b). The XRD patterns for powder samples are defined by broad bands as can be seen in Fig. 2a, which clearly confirm their amorphous nature, this result being in good agreement with those provided by STEM investigation.

The positions and widths of the powder samples XRD bands have been precisely identified by performing profile deconvolution using a Gauss function, after applying a baseline subtraction [7]. The two broad bands exhibited around 2theta = 28.2° and 52.8°, respectively, have been observed in all powder samples. These bands are generated by the short range order (SRO) in covalently networked materials, being attributed to the structural vitreous As_2Se_3 and $GeSe_2$ phases, corresponding to the 3.2 Å and 1.6 Å inter-planar d-spacing values [8]. The $Ge_{0.07}As_{0.07}Se_{0.86}$ and $Ge_{0.09}As_{0.09}Se_{0.82}$ powder samples have also revealed a third XRD band at lower 2theta angles, being more visible after deconvolution. However, the low angle bands were also clearly observable before deconvolution, appearing as a shoulder in the principal band of the patterns.

The low angle band of x=0.07 powder sample appeared at 19.29°, corresponding to scattering vector (Q) of 1.37 $Å^{-1}$. The scattering vector Q was calculated as 4 $\pi \sin \theta/\lambda$, where θ is the diffraction angle and λ is the X-Ray wavelength. The low angle band of x = 0.09 powder sample appeared at slightly higher 2theta angle and scattering vector, 19.68° and 1.38 $Å^{-1}$, respectively. These low angle bands represent the First Sharp Diffraction Peaks (FSDPs) and their presence is attributed to the existence of an intermediate range order (IRO) in the investigated materials. It seems that with the increase of Ge and As amounts up to x = 0.14 in the prepared chalcogenide powders, the FSPD disappears, thus the intermediate range order (IRO) is no longer present in the material.

Using the FSPDs data revealed by the two powder samples (x = 0.07 and x = 0.09), namely their scattering vector (Q) positions and Full Width at Half Maximum values (ΔQ), the repeating distance that is associated to the size of structural units (d-spacing) and the dimension of the region where the periodicity is preserved (L), have been calculated using the following formulas: $d = 2\pi/Q$ and $L = 2\pi/\Delta Q$ [9]. The $Ge_{0.07}As_{0.07}Se_{0.86}$ sample (ΔQ = 0.35 $Å^{-1}$) exhibited slightly higher d and L parameters of 4.58 Å and 17.94 Å, respectively, compared to those revealed by the $Ge_{0.09}As_{0.09}Se_{0.82}$ sample (ΔQ=0.36 $Å^{-1}$), 4.55 Å and 17.44 Å, respectively. This decrease could be associated with the increase in the Ge and As relative fractions used in the preparation of the three component system. However, based on the performed calculations, it can be assumed that in the investigated glasses there are microcrystalline domains with an ordered structure, with dimensions of about 17-18 Å.

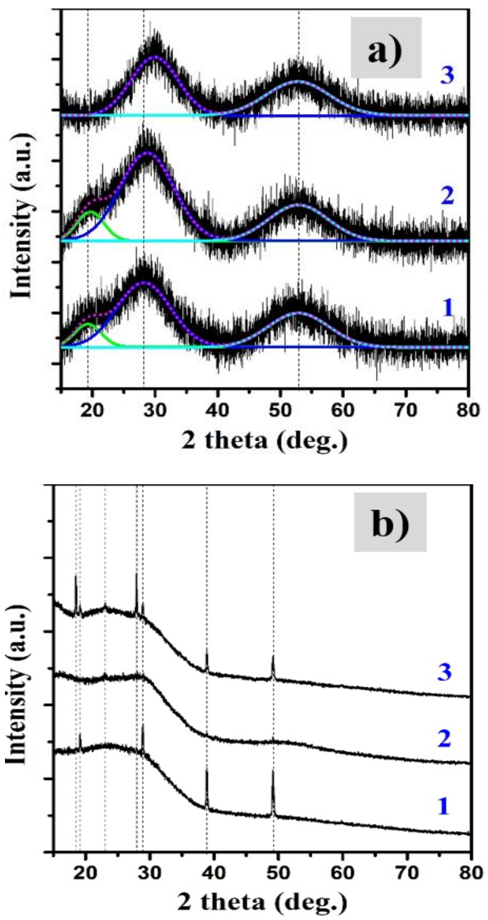

Fig. 2. XRD patterns exhibited by the (a) powder and (b) thin film $Ge_xAs_xSe_{1-2x}$ samples; x: 1 = 0.07, 2 = 0.09 and 3 = 0.14, respectively (color online)

Fig. 2b) displays the XRD patterns revealed by the $Ge_xAs_xSe_{1-2x}$ thin films. As can be clearly observed, the patterns of the films are also exhibiting sharp peaks compared to the powder samples which are described only by broad bands. These sharp peaks confirm the presence of some crystalline phases/fragments in the deposited materials, this result being in good agreement with the STEM data. The more intense and sharp peaks of the Ge-As-Se deposited films, suggests a stronger covalent network of the Ge-As-Se systems, made up also by clear crystalline phases, which are generated by the edge- and corner- interconnections of highly symmetric pyramidal ($As(Se_{1/2})_3$) and tetrahedral ($Ge(Se_{1/2})_4$) structural units [2].

In our case some phases of selenide and germanium selenide were also identified. That suggests that in the thin films composition are presented some crystalline incorporations (phases) of germanium selenide ($GeSe_2$), as well as in the studies [8]. In our case some selenide phases were also detected when analyzing the local bond structure as in the investigations of the $Ge_xAs_ySe_{1-x-y}$ glasses by X-ray photoelectron spectroscopy [10]. It was found the presence of the $GeSe_{4/2}$ tetrahedral, $AsSe_{3/2}$ pyramidal as well as the Se trimmers. It was also observed that the defect bonds rise with increase of the mean coordination number. In addition, X-ray diffraction data combined with modeling studies have shown that the most likely structure of a similar $Ge_{30}As_4S_{66}$ glass is based on a continuous random network connected so that dangling bonds in the structure are minimized with a minimum number of homopolar bonds [11].

3.3. Micro-Raman studies results

A detailed Raman study has been carried on to study the optical and structural properties of the $Ge_xAs_xSe_{1-2x}$ systems. Figs. 3 illustrate the micro-Raman spectra of $Ge_xAs_xSe_{1-2x}$ powder and thin films, respectively. As can be seen in Fig. 3a), b), the Raman signature of all the investigated samples, with a mean coordination number equal or smaller than 2.6, show overlapped bands, which cannot be clearly distinguished within 160 and 300 cm^{-1} spectral range. To precisely identify the positions of the peaks, the spectral regions of interest have been deconvoluted by using Voigt function, after applying a baseline correction.

Representative examples with deconvoluted Raman spectra for both powder and thin film $Ge_{0.09}As_{0.09}Se_{0.82}$ chalcogenides are illustrated in Fig. 3c) and d), respectively. As can be observed, the investigated samples, in both powder and thin film forms, are characterized by three main vibrational bands. Based on deconvolution results (Fig. 3c), the three main Raman peaks exhibited by the powder samples are located around 194 cm^{-1}, 238 cm^{-1} and 257 cm^{-1}, respectively.

The first peak located at 194 cm^{-1} could be attributed to the vibrations of the GeSe bonds within the $Ge(Se_{1/2})_4$ tetrahedral structural units. [12] The second band revealed around 238 cm^{-1} could be assigned to the presence of $As(Se_{1/2})_3$ pyramidal structural units and Se_n trimmers/chains [13, 10].

The third Raman peak shown at 257 cm^{-1} corresponds to the bond-stretching vibration of the disordered Se chains and rings [14]. The deconvolution results of the thin films (Fig. 3d) evidenced the presence of the same Raman bands as those exhibited by the powder samples, but with slightly shifted positions.

The first and third bands undergo a blue shift to lower wavelengths, from 194 cm^{-1} to 195 cm^{-1}, and from 257 cm^{-1} 261 cm^{-1}, respectively, while the second band suffers a red shift, from 238 cm^{-1} to 234 cm^{-1}.

The Raman spectra of $Ge_xAs_xSe_{1-2x}$ powder and thin films show that with the increase of Ge concentration, the intensity of the first main peak (around 194 cm^{-1}) increases, most likely as a result of the increase in the density of the $Ge(Se_{1/2})_4$structural units. The Full Width at Half Maximum (FWHM) of the vibrational band located at 194 cm^{-1} also increases with the increase of Ge concentration, from 14 cm^{-1} for x=0.05 up to 27 cm^{-1} for x=0.30. On the other hand, the intensity of the third Raman band (around 257 cm^{-1}) decreases with the increase of the Ge relative fraction incorporated in the prepared systems, suggesting a decrease in the disordered Se chains and rings number.

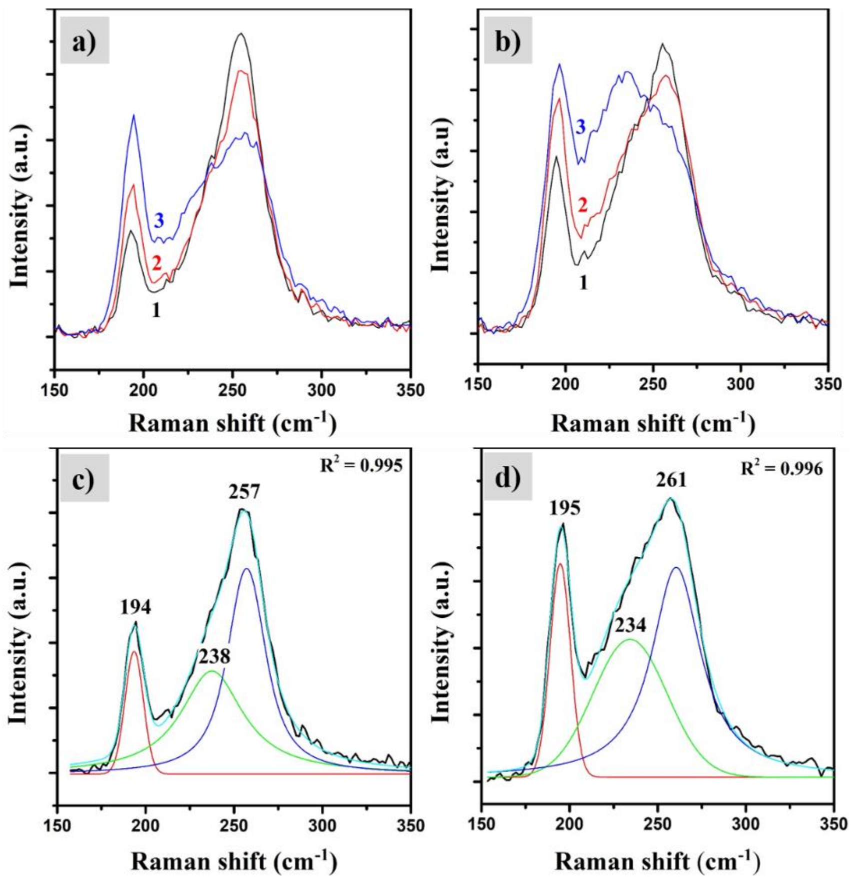

Fig. 3. Micro-Raman spectra revealed by (a, c) powder and (b, d) thin film x = 0.07, 0.09 and 0.14 $Ge_xAs_xSe_{1-2x}$ samples and their representative deconvolution spectra (color online)

A reported Raman study of the Ge-Se compounds has shown a reduction in the scattering strength of Se chain modes near 260 cm^{-1} and an enhancement in scattering strength of the vibration mode around 234 cm^{-1}, which could indicate a phase separation in these materials.

It was also observed that the position of the peak at 194 cm^{-1}, attributed to the tetrahedral $GeSe_{4/2}$ units, remains almost constant up to 2.5 coordination numbers (Z). For higher Z, the band slightly shifts to lower wavenumbers. At high Ge and As at. % concentrations, the vibration mode at 257 cm^{-1} disappears, as a result of the complete replacement of Se by Ge and As in $Ge_xAs_xSe_{1-2x}$ chalcogenide glasses.

4. Conclusions

The amorphous nature of the powder samples and the presence of some crystalline fragments in the deposited thin films have been shown by HR-STEM and XRD investigations. Moreover, the XRD data through the presence of FSDPs in some of the investigated samples patterns, unraveling their intermediate order range (IOR) organization. It was shown that FSDP depends on the three-component system composition. At higher x values (x=0.14), the FSDP disappears.

The micro-Raman investigations revealed the presence of three main vibration modes for the investigated systems, which correspond to As-Se, Ge-Se bonds and Se chains and rings. It was shown that the increase of Ge concentration leads to an increase in the density of the $Ge(Se_{1/2})_4$ structural units.

Based on all these results, a thorough insight in the structural arrangements of different $Ge_xAs_xSe_{1-2x}$ compositions is provided, which could enable the control of these systems' physical properties in order to make them suitable for different applications, such as phase change memory devices.

Acknowledgement

This work was financially supported by the project ANCD 20.80009.5007.14 and also by the Romanian Ministry of Education and Research, under the following ECSEL-H2020 Projects: PIn3S—Contract no. 10/1.1.3H/03.04.2020, POC-SMIS code 135127 and BEYOND5—Contract no. 12/1.1.3/31.07.2020, POC-SMI_S code 136877.

References

[1] M. Popescu, A. Andriesh, V. Ciumash, M. Iovu, S. Shutov, D. Tsiuleanu, Editura Stiintifica, Bucuresti, 1996, Reprinted by Editura Stiinta, Chisinau, ISBN: 5-376-01514-9, (In Romanian: Fizica sticlelor halcogenide) Edition: Bucuresti-Chisinau.
[2] S. R. Elliott, Physics of Amorphous Materials, Longman, London, 2-nd edition, (1990).
[3] R. Golovchak, O. Shpotyuk, M. Iovu, A. Kovalskiy, H. Jain, J. Non-Cryst. Solids **357**(19-20), 3454 (2011).
[4] M. S. Iovu, S. A. Sergeev, O. V. Iaseniuc, Optoelectron. Adv. Mat. **12**(7-8), 377 (2018).
[5] M. S. Iovu, O. V. Iaseniuc, Optoelectron. Adv. Mat. **12**(9-10), 563 (2018).
[6] A. Zakery, S. R. Elliot, J. Non-Cryst. Solids **330**(1-3), 1 (2003).
[7] H. F. Poulsen, J. Neuefeind, H.-B. Neumann, J. R. Schneider, M. D. Zeidler, J. Non-Cryst. Solids **188**, 63 (1995).
[8] Toshihiro Nakaoka, Hiroki Satoh, SaoriHonjoand Hideo Takeuchi, AIP Advances **2**(4), https://doi.org/10.1063/1.4773329 (2012).
[9] A. I. Isaev, S. I. Mekhtieva, Kh. I. Mamedova, R. I. Alekberov, Physics and Chemistry **46**(1), 41 (2020).
[10] M. Olivier, J. C. Tchahame, P. Němec, Optical Materials Express **4**(3), 525 (2014).
[11] S. Mamedov, D. G. Georgiev, Tao Qu, P. Boolchand, J. Physics: Condensed Matter. **15**, S1573 (2003).
[12] P. Boolchand, M. Jin, D. I. Novita, S. Chakravarty, Journal of Raman Spectroscopy **38**, 660 (2007).
[13] Tao Qu, D. G. Georgiev, P. Boolchand, M. Micoulaut, Mat. Res. Soc. Symp. Proc. **754**, CC8-12 (2003).
[14] R. P. Wang, A. Smith, A. Prasdad, D. Y. Choi, B. Liuter-Davis, J. Appl. Phys. **106**, 043520-5 (2009).

*Corresponding authors: miovusel@gmail.com, oxana.iaseniuc@gmail.com